STED and RESOLFT Fluorescent Nanoscopy

Andreas Bodén, Francesca Pennacchietti, and Ilaria Testa

Contents

1 Introduction 202
2 Light-Induced Reversible State Transitions 205
2.1 Reversible Electronic Transitions: Stimulated Emission 206
2.2 Reversible Molecular Transitions 208
3 Adaptive and Smart Scanning of the Illumination 211
4 Optimized Patterns and Adaptive Detection 213
5 Parallelization 214
5.1 Parallelized STED 216
5.2 Parallelized RESOLFT 217
5.3 Digital Pinholing of Camera Data 222
6 STED and RESOLFT for Live-Cell Imaging 222
7 Challenges and Outlooks 226
References 228

Abstract Fluorescence microscopy is an invaluable tool in cell biology to investigate the functional, structural, and dynamical properties of biological specimens. For a long time, the resolution of fluorescence microscopes was thought to be fundamentally limited by diffraction. According to Abbe's law of diffraction, published in 1873, the smallest spatial details accessible with visible light are defined only by the optics of the microscope, i.e., numerical aperture and the wavelength of the light. However, the last 25 years of research have shown that it is possible to investigate even smaller structures using only visible light. This chapter covers the basic principles of coordinate-targeted switching techniques, a family of super-resolution microscopy methods. Furthermore, it provides an overview of the state-of-the-art strategies to push their ability toward faster and more efficient imaging of living cells and tissue.

A. Bodén, F. Pennacchietti, and I. Testa (✉)
Science for Life Laboratory, KTH Royal Institute of Technology, Stockholm, Sweden
e-mail: andreas.boden@scilifelab.se; francesca.pennacchietti@scilifelab.se; ilaria.testa@scilifelab.se

R. Šachl, M. Amaro (eds.), *Fluorescence Spectroscopy and Microscopy in Biology*,
Springer Ser Fluoresc (2023) 20: 201–232, https://doi.org/10.1007/4243_2022_35,
Published online: 3 January 2023

Keywords Fluorescence nanoscopy · Live-cell imaging · Photoswitching · Parallelization · Smart scanning

1 Introduction

Fluorescence microscopy is an invaluable tool for the investigation of spatial distribution and dynamics of cellular and tissue structures in biological samples. Fluorescence allows reaching high contrast and selective labelling of proteins of interest in a live-cell compatible manner. Two main strategies can be distinguished in fluorescence microscopy, according to the way the image is created. In the case of widefield microscopy, the whole sample is excited through an even and extended illumination, and the fluorescence is collected at once with your eye or on an imaging detector (Fig. 1a). Alternatively, in scanning approaches, the sample is probed point-by-point using a sharply confined spot of excitation light. To enhance the image quality of a scanning microscope, a pinhole is placed in the image plane of the detection path to spatially filter out and select primarily the light emitted from the focal plane of the sample (confocal microscope, Fig. 1b). Confocal microscopy introduces optical sectioning and increased spatial resolution compared to widefield approaches. Widefield systems can however image significantly faster than scanning microscopes on extended fields of view (FOV) and are simpler and cheaper to build and maintain. Both widefield and scanning microscopes are limited in spatial resolution by the wavelength of light, as first realized by Ernst Abbe in 1873 when he formulated the theory behind the diffraction limit [1]. The wave nature of light means that it cannot be focused to a spot smaller than roughly half its wavelength. This characteristic consequently sets a limit on the size and shape of the so-called point spread function (PSF) of a microscope, which describes the image of an isolated emitting point in the sample. If two adjacent emitting points are distanced significantly closer than the size of the PSF and imaged through an optical system, their PSFs will overlap and they will thus not be resolvable in the image.

Super-resolution fluorescence microscopy techniques emerged in the late 1990s, pushing the resolution beyond the diffraction limit imposed by the wave nature of light. The key to surpassing the diffraction limit lies in the possibility to switch a fluorescent molecule between an on and an off state [2–4] (Fig. 2a). This can be done either in a deterministic way, using the on/off switching to reduce the effective PSF, or in a stochastic way, by recording the emission of many individual molecules within a diffraction-limited spot one at a time (single molecule localization microscopy, SMLM) [5–7].

This chapter will focus on the deterministic methods, alternatively called coordinate-targeted switching approaches, since they rely on the point-by-point investigation of the sample typical of a scanning microscope. The optical suppression of the fluorescence can be achieved either by STimulated Emission Depletion (STED) [8, 9] or more generally by Reversible Saturable OpticaL Fluorescence

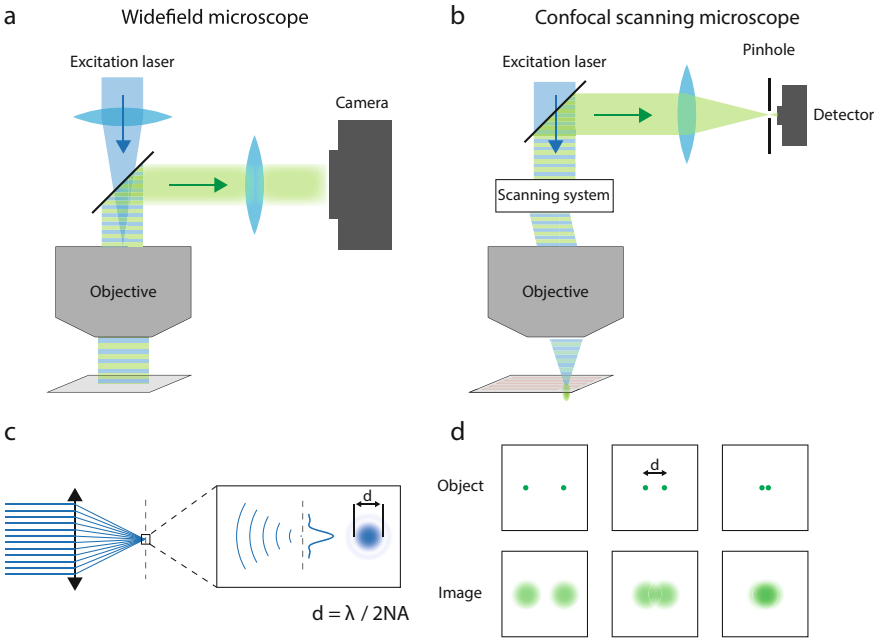

Fig. 1 Fluorescence microscopy. (**a**) A widefield fluorescence microscope illuminates the whole sample with excitation light, creating fluorescence emission that is imaged through the objective onto a camera. (**b**) An image can also be generated by sequentially scanning a focused probing beam over the sample, at each point measuring the amount of emitted fluorescence. In a confocal scanning microscope, the detected light is also passed through a pinhole to reject emission from out-of-focus planes. (**c**) The wave nature of light means that it cannot be focused onto an infinitesimally small spot. The smallest achievable focal point is around half the wavelength of the light that is focused. This limit is called the diffraction limit. (**d**) The image of an emitting point is called the point spread function (PSF) and its size is limited by the diffraction limit. Two adjacent emitting points can only be resolved if they reside further away from each other than about half the size of the PSF of the imaging system

Transitions (RESOLFT) [10–12]. STED is based on optically perturbing the electronic transition pathway that generates the fluorescence, and can therefore act on the ps-ns scale (Fig. 2d). In RESOLFT, the fluorescence properties of the molecule changes in response to a perturbation of its chemical configuration (Fig. 2e). Since the dark states involved in RESOLFT have a longer lifetime, the switching is notably slower (μs-ms scale) but requires magnitudes lower illumination intensities. Starting from a conventional confocal microscope, super-resolution can be achieved using STED or RESOLFT by superimposing a patterned illumination on top of the excitation illumination. The patterned illumination suppresses fluorescence emission from the outer regions of the diffraction-limited excitation spot and allows fluorescence emission only from the very central point where the suppressing light is zero. In this way, the effective excitation spot is shrunk, giving a finer probing of the sample structure (Fig. 2f). Expanding scanning systems to these super-resolution

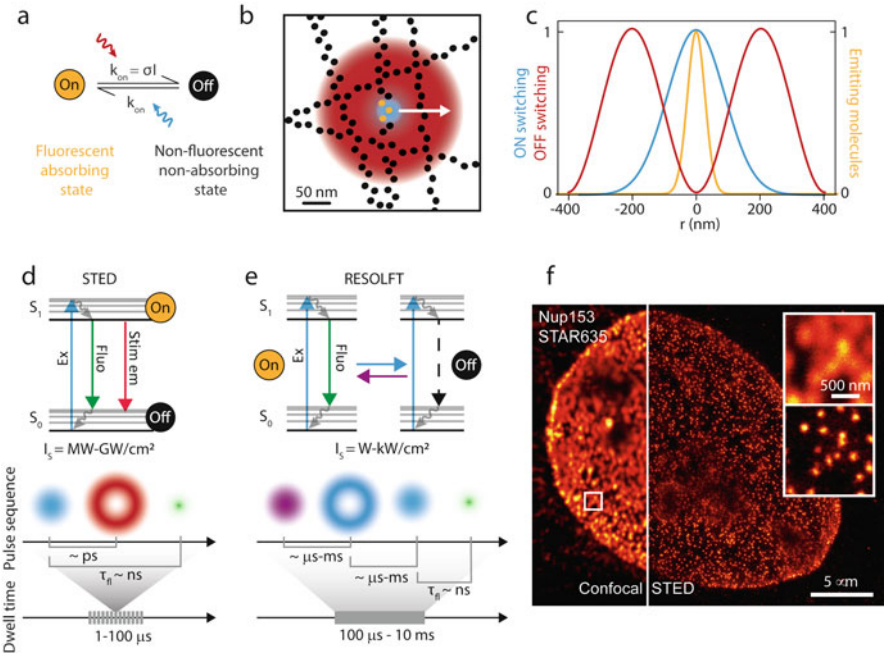

Fig. 2 Coordinate-targeted nanoscopy. (**a**) Illustration of the on/off switching between a fluorescent and a non-fluorescent generic molecular state. The on-to-off transition is induced by red light, while the off-to-on is induced by blue light. (**b**) Spatial distribution of the light and the state distribution of the molecules in the foci of a coordinate-targeted switching point-scanning microscope in 2D and (**c**) in 1D. To optimize on-state confinement (orange line), the minimum of the off-switching light (red line) should be exactly at the maximum of the on-switching (blue line). (**d**) Jablonski diagram illustrating electronic transitions of the standard pathway of fluorescence emission and how stimulating emission can inhibit the emission of fluorescence by forcing the molecule to emit the excess energy as stimulated emission photons. Below the state diagram is an illustration of the pulse sequence and dwell time for a STED recording. In the pulse sequence, the time delay between the different pulses and emission is highlighted. (**e**) Diagram illustrating a molecular transition where the molecule can instead be switched between two metastable molecular states, referred to as on and off state. The probes can be switched between the two states through illumination with different wavelengths of light. Below the state diagram, an example RESOLFT pulse scheme and dwell time is shown on a time scale. (**f**) Example of STED imaging. Confocal and STED images of the nucleus of a U2OS cell with inset showing zoomed-in area. The nuclear pore complex protein Nup153 has been labeled with Abberior STAR635P. Scale bars: 5 µm, and 500 nm, respectively

implementations however also adds significant complexity and comes with new challenges, both from an optical engineering perspective and in terms of sample preparation and label design.

STED and RESOLFT approaches were first introduced in a point-scanning implementation, where images are acquired by sampling over the FOV using a single probing spot. This adds a dependency between the temporal resolution and the imaged area (or volume) since the dwell time at each position is multiplied with

the number of sampling points. Thus, point-scanning microscopy methods reach a high temporal resolution for small areas and volumes but imaging time quickly increases when scaling up the FOV. To overcome these limitations, multiple approaches to further increase the imaging speed have been proposed and demonstrated since the introduction of the methods, including minimizing the recording time and illumination doses by using smart scanning or by introducing light patterns to parallelize the acquisition. Smart scanning refers to systems where a single excitation spot is adaptively scanned over the sample, meaning that the scanning speed or illumination intensities are modulated in real time during the scan. Therefore, scanning of regions of the sample which do not contain structures of interest can either be completely avoided or illumination levels can be adapted to the structure. This increases the speed and/or lowers the illumination dose in an adaptable way for each FOV and its biological content. Smart or adaptive scanning systems have been demonstrated to improve performance both in STED and RESOLFT [13, 14]. Another approach to increase acquisition speed is to instead utilize the concept of parallelization where a large array of confined PSFs is generated in each illumination sequence. In these methods, the temporal resolution does not scale linearly with the FOV size, since the total sampling area is instead determined by the distance between two adjacent points in the array (which can be as close as 250 nm, limited only by diffraction). As a consequence, parallelized systems have a clear advantage when imaging larger areas.

In this chapter, we will describe the underlying concepts of STED and RESOLFT microscopy, and outline their strengths and limitations. In particular, we will review the approaches and ideas demonstrated to increase the imaging speed and decrease the illumination dose with the main goal of increasing their compatibility with live-cell imaging over extended periods of time.

2 Light-Induced Reversible State Transitions

Many state transitions can be used as reversible on/off switches. Their suitability for coordinate-targeted switching techniques depends on how efficiently molecules can be switched to a certain state at a specific time and be reversibly brought back to the original state with minimal loss. This translates into spatiotemporal control of the saturation of state populations within the fluorophore population which is necessary for successful imaging. In practice, the biological application will lend itself better to the use of one type of transition over another, as the application sets the requirements on illumination, light source, recording time, photobleaching, and imaging environment. Regardless of the nature of the transition, the effective excitation spot will be given by the equation:

$$d = \frac{\lambda}{2\mathrm{NA}} \frac{1}{\sqrt{1 + I/I_S}} \quad (1)$$

where the intensity of saturation for the on-to-off transition is $I_S = k_{\mathrm{on}}/\sigma_{\mathrm{off}}$, with σ_{off} being the molecular cross-section for the transition and k_{on} accounting for the competing process that restores the initial fluorescent state [15]. The saturation intensity reports the intensity required to suppress the fluorescence to half its initial level and it is the key to obtaining the spatially sub-diffracted confinement of emitting molecules.

2.1 Reversible Electronic Transitions: Stimulated Emission

Following excitation from the ground state to the excited state, a fluorophore can release energy through spontaneous fluorescence emission or thermal relaxation. The return to the ground state can, alternatively, be induced by stimulated emission in an interaction with incoming photons. Illumination with light in which the photons have an energy equal to the energy gap between the excited and ground state will drive the electrons back to the ground state, resulting in the emission of photons of the same energy as the stimulating illumination, as illustrated in Fig. 2d. In STED, therefore, stimulated emission represents a competing process to fluorescence emission, effectively able to deplete the molecules from the excited state and thereby suppress the spontaneous fluorescence emission. Commonly used STED microscopes feature an illumination beam shaped like a doughnut to induce stimulated emission (depletion beam) overlapped onto a Gaussian-shaped beam of light used for fluorescence excitation. In the center, only the excitation light is present as the doughnut features a local "zero" here (Fig. 2c), and the molecules residing here will thus emit fluorescence. Instead, on the crests of the doughnut where the intensity of the STED beam is higher than the saturation level, I_s, the stimulated emission will prevail over fluorescence emission, effectively turning off the molecules in this peripheral area.

To efficiently drive the molecules to the off state, the stimulated emission transition has to outcompete spontaneous fluorescent emission, which has a lifetime of a few nanoseconds (1–5 ns). Combined with the low stimulated emission cross-section ($\sigma \approx 10^{-16}$ cm^2), this translates into a requirement of high photon flux ($I_s \sim$ MW–GW/cm^2) to achieve saturation of the on-to-off transition.

The relatively high intensity required by the STED beam sets specific demands on the fluorescent probes [16–18]. The main parameter for a probe to perform well in STED microscopy is photostability, meaning the ability of the probe to withstand several excitation-depletion cycles without significant photobleaching. The depletion wavelength depends on the emission spectrum of the fluorophore, and moving it toward the peak of emission gives a larger cross-section and therefore reduces the STED power needed [19, 20]. However, to avoid direct excitation by the depletion

beam and to minimize interference with the fluorescence window, the depletion wavelength is generally moved to the red tail of the emission spectra. Even in such optimized depletion conditions, the STED image quality can be compromised by the interference of the STED beam with other photophysical pathways. This can lead to excited state absorption [21, 22] which, in turn, can result in a higher probability of bleaching.

Stimulated emission is a general process universal to all fluorophores. As such, STED has been demonstrated with many fluorophores of different nature, e.g., organic molecules [16, 23], fluorescent proteins [24–26], and inorganic nanocrystals [27–29] (e.g., nanodiamonds, quantum dots, and lanthanide upconversion nanoparticles). Besides matching the photophysical parameters optimal for STED imaging, the choice of probe is also linked to its biocompatibility. Cytotoxicity can arise from the intracellular oligomerization and aggregation of probes, and the high illumination power can induce photothermal effects around the probe as well as the formation of free radicals and singlet oxygen molecules. It is difficult to absolutely predict and directly detect the damage induced during imaging [30, 31]. Therefore, it is often estimated by assessing cell viability before and after the imaging experiment. Phototoxicity is highly dependent on the irradiation wavelength, therefore a common strategy is to shift the illumination to the red region of the spectra. This also has the additional advantage of being less susceptible to scattering and creating less autofluorescence, thus increasing the possible penetration depth. Labeling strategies used for live-cell and in vivo STED microscopy rely on genetically encoded markers like fluorescent proteins; self-labeling protein tags [32–35] (SNAP-, HALO- or CLIP-tags) or unnatural aminoacids [36] combined with cell-permeable dyes; or small cell-permeable molecules with high labelling specificity that can be for example drug-based or lipid-based (e.g., NileRed and SiR-Actin) [37].

The nature of the STED process and in particular the need to act within the fluorescent lifetime of the fluorophore sets general requirements on the hardware used in STED microscopes [22]. STED lasers need to deliver high illumination power to the sample during the lifetime of the excited state and thus be precisely timed after the excitation (delay in the order of ~ps to allow relaxation to the lowest excited state). Pulsed lasers with picosecond pulse widths match these power (MW–GW/cm^2) and time (~500 ps) requirements for optimal depletion. The fast time scale of stimulated emission depletion directly translates into fast imaging times. Pixel dwell times in STED microscopy can vary from 1–300 μs depending on the fluorophore brightness and density. This requires a fast and precise scanning system, often based on galvanometric mirrors, resonant scanners [38], or electro-optical scanners [39]. Additionally, the fast scanning of STED systems also requires fast detectors and electronics able to record and distinguish photons from adjacent scanning points. Common detector types for STED microscopes are, for example, photo-multiplying tubes (PMTs), avalanche photodiodes (APDs), or single-photon avalanche diodes (SPAD).

2.2 Reversible Molecular Transitions

RESOLFT encompasses all the coordinate-targeted super-resolution approaches that rely on metastable or long-lived fluorescent and non-fluorescent states, which can be reversibly and efficiently populated upon illumination with specific wavelengths. The use of molecular transitions between metastable states with long lifetimes, such as isomers, decreases the intensity required since the transitions and population saturation do not have to be induced on the nanosecond time scale. Compared to using electronic transitions, the intensities used while imaging can be decreased by several orders of magnitude. For example, in states with lifetimes on the microsecond timescale, the intensity required for saturation is on the order of a few W/cm^2.

RESOLFT techniques set strong requirements on the fluorescent label, especially in terms of switching kinetics and photobleaching resistance [40]. In STED microscopy, the use of electronic transitions on the nanosecond timescale makes the process quasi-instantaneous. In RESOLFT, the kinetics between the on and the off state reside within the microsecond–millisecond timescale and therefore directly influence the image recording time negatively (Fig. 1e). To be suitable for RESOLFT imaging, the conformational changes that underpin photoswitching needs to withstand many cycles. For example, to be able to acquire an image with an expected resolution of 50 nm in the focal plane, a step size of 25 nm is needed (according to Nyquist-Shannon sampling theory). Assuming that proteins within a 200×200 nm^2 area are switched on in every illumination cycle, the proteins will need to cycle at least $(200/25)^2 \approx 60–70$ times without a significant loss in fluorescence to allow for an image to be acquired. The ability of a probe to be photoswitched many times without significant loss of fluorescence is referred to as fatigue resistance.

Reversible on-off switching mechanisms can be found in reversibly photoswitchable fluorescent proteins (RSFPs) and organic photochromic fluorophores (Fig. 3). In GFP-like proteins, reversible photoswitching is generally a result of a photoinduced isomerization coupled with a protonation/deprotonation of the chromophore [41]. Three types of photoswitching can be identified according to how light controls the switch: positive, negative, and decoupled. The three types and their response to illumination schemes are illustrated in Fig. 3a–c.

In negative switchers, the excitation wavelength also induces off-switching (Figs. 1e and 3a). The coupling of the excitation and off-switching wavelength imposes a sequential recording scheme where, at first, an ensemble of molecules is switched to their emitting states. Subsequently, a spatially patterned light featuring a minimum in the center switches off all the molecules in the periphery and leaves only the ones in the center able to emit. At last, those are excited and their fluorescence is induced upon illumination with a third beam of the same wavelength (Fig. 3a). Negative RSFPs have varying off-switching kinetics affecting the dwell time used for imaging, from tens of μs to ms. For fast switchers like rsEGFP2 or Dronpa2, the dwell time is generally 300 μs in a point-scanning recording and 3 ms in a parallelized system where lower intensities are generally used. The most

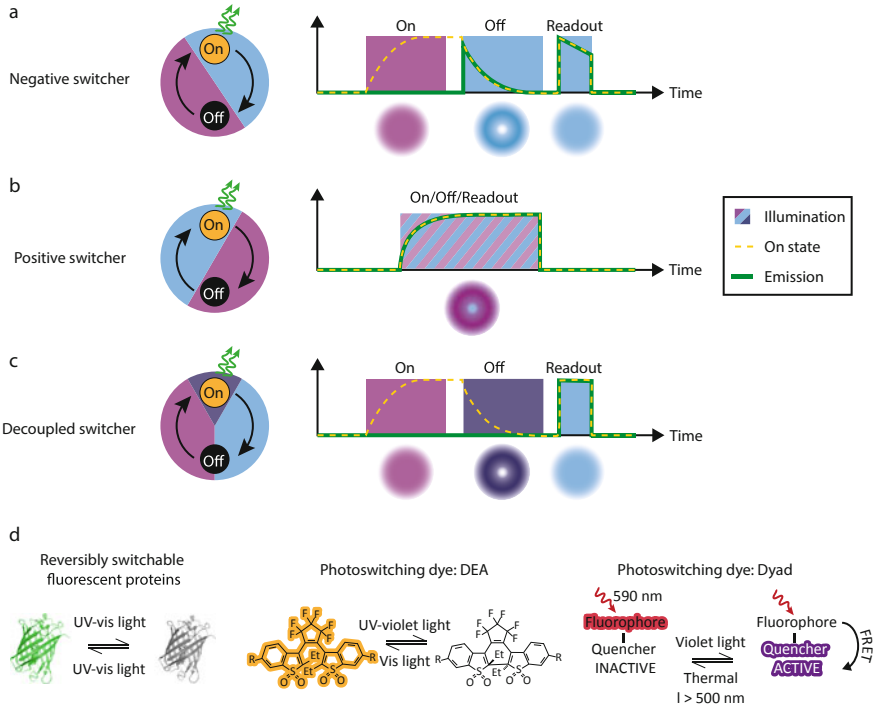

Fig. 3 Reversibly switchable probes. Example of photoswitching behavior and related effects on the pulse scheme used for RESOLFT. (**a**) Negative switchers are fluorescently excited by the same wavelength as that which causes them to switch off. (**b**) Positive switchers are fluorescently excited by the same wavelength as that which switches them on. (**c**) Decoupled switched are switched on and off and are excited by three separate wavelengths. (**d**) Example of used switching mechanisms for RESOLFT. In reversibly switchable fluorescent proteins, the switch is linked to a *cis/trans* isomerization combined with a protonation/deprotonation step or by a rearrangement of the hydrogen network. Among the photoswitching dyes, some of the molecular mechanisms used are either directly switching the dye between an "open" and a "closed" form or indirectly using this switching to enable or impair the fluorescence of a covalently-linked dye. The molecular structure and schemes are readapted from the original publications [59, 60]

common types of negative switchers have excitation maxima in the blue (~488 nm) and on-switching in the UV–violet. The ability to completely cycle a population within hundreds of microseconds together with their ability to withstand thousands of switching cycles made rsEGFP2 [12] and Dronpa2 [42] fundamental for the development of the RESOLFT concept and the possibility to achieve the best trade-off between temporal and spatial resolution. Additional variants such as rsGreen [43] and rsFolder [44] were also developed to enhance the expression levels in mammalian and bacterial cellular systems. The need for new and brighter labels led to the further development of the GMars family [45, 46], whose biphasic photobleaching trend can be used for prolonged timelapse imaging. The development of the rsGamillus family [47], instead, extended the imaging to biological

processes in more acidic pH compared to the physiological one. Furthermore, the use of photoswitching mechanisms outside the GFP superfamily and into the bacterial photoreceptors, such as the LOV domain of YtvA from *Bacillus subtilis*, adds to the list a smaller oxygen-independent alternative compatible with anaerobic environments [48].

For the positive switchers, the excitation wavelength is coupled to the on-switching path while the off-switching is driven with violet light (Fig. 3b). All the reported positive switchers, such as Padron [49] and Kohinoor [50], are in the green spectral range, with on-switching and excitation around 488–500 nm and off-switching in the UV–violet range. With the faster switching speed and the different dependency on the wavelengths exhibited by the newly developed Padron2, Konen et al. demonstrated point-scanning RESOLFT imaging with illumination patterns superimposed both spatially and temporally and with pixel dwell times of ~500 μs [51].

For the decoupled switchers, the switching is fully decoupled from the excitation wavelength (Fig. 3c). The RSFP Dreiklang is switched on and off by illumination at ~365 nm and ~405 nm, respectively, while the excitation wavelength is at ~515 nm [52, 53]. In contrast to the other groups, the switching is the result of a reversible hydration/dehydration reaction that modifies the chromophore. In terms of imaging, these switching properties allow maximization of the photon budget of the protein, potentially increasing the SNR. However, the switching speed of current decoupled switchers is significantly slower and has so far required pixel dwell times of ~20–50 ms, thus liming their use for dynamic live-cell imaging.

The reported switching mechanisms are predominantly in the green region of the spectra and require the use of UV–violet light to a varying extent. To reduce any potentially phototoxic effects of the shorter wavelengths and thereby enhance the live-cell compatibility of RESOLFT, there is a continuous push to develop probes in the red region of the spectra. Examples of variants successfully used in RESOLFT are asFP595 [10] and rsCherryRev1.4 [54]. They are negative switchers, with excitation maxima in the orange (~590 nm) and a broad on-switching range between UV–violet and green (400–510 nm). The newly reported red fluorescent protein variants of rsFusionRed show a sevenfold decrease in off-switching time, allowing imaging speeds compatible with living cells and enough photostability to follow their dynamics over multiple frames [55].

Different photoswitching strategies have been identified also in synthetic dyes (Fig. 2d). The covalently-linked dye pair of Cy3 and Alexa647 can act as an organic photoswitcher, using the long-lived non-fluorescent state of the dye in a thiol buffer solution and the possibility to revert it by a different wavelength of light [56]. Fluorescence bis-sulfone diarylethenes have also been used for RESOLFT [57–59]. These compounds present an “open” and “closed” chemical form of the chromophore and upon illumination with UV–visible light (350–405 nm), they switch to the fluorescent isomer. Alternatively, the fluorescence of a dye can be modulated by a covalently-linked photoswitchable quencher [60]. This strategy employs a different class of photoswitchers called spironaphthoxazines, which can switch from a yellow spiro form to a deep violet merocyanine form upon 405 nm

illumination, enabling Förster energy transfer and consequently quenching of the second fluorophore. Even if brighter than fluorescent proteins, the overall performance of synthetic dyes in RESOLFT microscopy is limited. The major challenges are still photobleaching, reduced number of cycles, and often the need for UV light or a specific environment for optimized switching. Nevertheless, the possibility to open up the technique to new labeling approaches for living cells (like SNAP-Tag or HaloTag technologies) is an area of interest in the field.

From the hardware point of view, the nature of the transitions used in RESOLFT eases the requirement of power and time compared to STED microscopes, and thus the requirements of the lasers. The much lower peak intensities (kW–W/cm^2) required for molecular switching are compatible with continuous wave (CW) lasers. A key technical aspect is also the possibility to digitally modulate the illumination on the μs-ms timescale, achievable both through commercial CW lasers or acuosto-optic modulators. The different pulse sequences that have been implemented in RESOLFT are summarized in Fig. 3.

3 Adaptive and Smart Scanning of the Illumination

In a point-scanning system, an image is acquired by scanning a probing beam over the FOV to be imaged, point-by-point and line-by-line (Fig. 4a). The residence time of the beam in each pixel is called the dwell time, t_s, while the step size from one point to the other (corresponding to the final pixel dimension) is called the scanning step, Δx. In the context of a single-point-scanning system, the imaging speed is determined by the number of scanning points, n_s, required to construct the image and the dwell time required to measure at each scanning position. The number of scanning points in turn depends on the scanning step size and the size of the imaged field of view (l_{fov}), while the dwell time required to collect sufficient signal depends on the illumination power, switching kinetics, brightness, and labelling density. In most traditional systems, the aforementioned imaging parameters, n_s, t_s, and l_{fov}, are set to fixed values before image acquisition begins. This means that the same parameters will be used for every scanning point, regardless of the sample properties at that point. Consider, for example, a large sample area in which labeled structures of interest are sparsely dispersed. Large regions of the area will not contain structure and thus not generate any signal, but will still be imaged using the same parameters as the regions containing structure. This results in unnecessarily long acquisition times and large total illumination dose also to samples containing small or sparse structures (Fig. 4a). Smart scanning or adaptive illumination systems feature a more flexible and sample-dependent scanning scheme, where the dwell times or illumination intensities are adjusted depending on the properties of the sample in the currently scanned region (Fig. 4b–c).

Adaptive illumination has been used to decrease the illumination dose of STED microscopy (Fig. 4b). In adaptive illumination STED microscopy, the power of the STED laser is modulated during the scan in response to the structure of the sample.

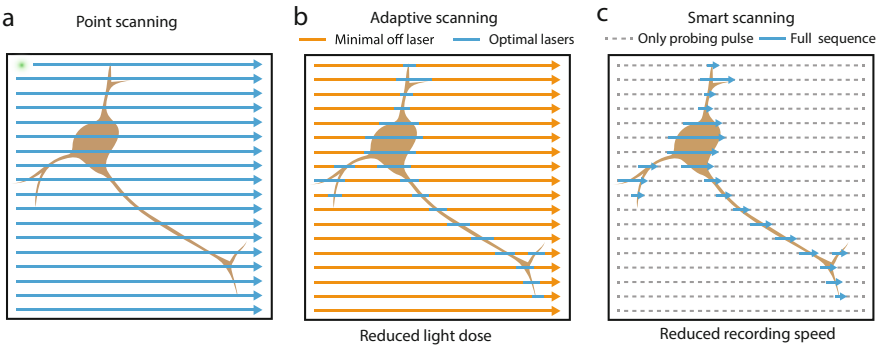

Fig. 4 Point-scanning approaches. (**a**) Conventional point scanning. By scanning a probing focal spot over the sample in a raster-scanning geometry and detecting the amount of fluorescence generated at each point, a point-scanning microscope builds up an image of the sample pixel-by-pixel. According to the Nyquist-Shannon criteria, the scan step should be no more than half the expected resolution. Therefore, if a 10× resolution increase is expected over a diffraction-limited image, the scanning steps required are 100× more in a 2D image. This leads to a significantly slower recording time and increased light dose on the sample. The size of the probing focal spot determines the level of detail i.e. the resolution of the image. (**b**, **c**) Point-scanning microscopy can be made more efficient by implementing adaptive or smart scanning approaches. (**b**) Adaptive scanning refers to the adaptation of illumination intensities to the sample structure. A weak intensity is used as an initial probe. When sample structure is detected, the illumination powers are increased to optimize image quality at regions containing structure of interest. (**c**) Smart scanning approaches also adapt the temporal pulse sequence at each pixel to the sample, essentially skipping over pixels that do not generate significant signal when probed with a probing pulse. Adaptive scanning minimizes the illumination dose on the sample and smart scanning additionally decreases the required scanning time

The sample is scanned with a diffraction-limited excitation spot with constant intensity. As long as the excitation spot does not generate fluorescence, no STED illumination is applied. When fluorescence exceeds a certain threshold the STED beam is activated (RESCue-STED) [61]. In DyMIN (Dynamic Intensity Minimum), the STED beam is instead switched on at increasing power the higher the fluorescence detected, and therefore the structure of interest more centered in the recorded area. This strategy minimizes the STED illumination, using the STED beam only when and at the intensity needed to maximize information instead of always at the maximum level independently from the characteristics of the sample. DyMin has been tested on periodic actin structures as well as the gephyrin clusters at inhibitory synapses of rat hippocampal neurons [14], with a reduction of total light dose on the sample up to 45-fold. Moreover, the more efficient illumination scheme allows the use of longer pixel dwell times without bleaching, enabling imaging at higher signal-to-noise ratio compared to conventional scanning.

When the regions of interest are within the scale of the diffraction limit, the concept of sample-dependent scanning can be adapted accordingly. In MINFIELD [62], a low-resolution image of a sparse sample is used to localize small substructures and define small regions of interest (~100 × 100 nm^2) that are sequentially

imaged with the STED beam active. Since the region of interest containing the structure is smaller than the size of the STED beam (central zero FWHM ~ 280 nm), MINFIELD minimizes the exposure of fluorophores to STED illumination as they will not see the maximum intensity of the doughnut crest.

These approaches are efficient in decreasing the light dose to the sample. A further improvement toward live-cell compatibility is to speed up the acquisition with smart scanning approaches. Smart scanning implementations in RESOLFT involve using a short initial probing pulse to detect the presence of any fluorescent structure [13] in a specific scanning step. If the probing pulse generates a low signal, the region is ignored and the scan rapidly moves on to the next scanning position. If the probing pulse generates sufficient photons, the region is considered to be of interest, and the full RESOLFT pulse scheme is applied at the current scanning point (Fig. 4c). This smart scanning approach saves time in the acquisition by not dwelling on pixels that do not add information to the image, and the speed-up depends on the type of structure being imaged. The method reaches up to 6 times faster recordings and is an especially efficient approach when imaging, for example, neuronal protrusions or sparse point-like structures, where only a small fraction of the pixels (15%) in the final image will contain relevant information. Using smart scanning RESOLFT, Dreier et al. show peroxisome dynamics in small fields of view at imaging speeds of 2–5 Hz and mitochondria membranes at imaging speeds of 27 Hz, essential to remove motion artifacts. Furthermore, it was shown that the illumination dose could be decreased by 70–90% [13] since regions of the sample not containing labeled structures are not exposed to the RESOLFT imaging scheme but only to the probing illumination.

The use of fast scanning devices, like electro-optic deflectors (EODs), introduces the possibility of pixel hopping also in STED. FastRESCue STED [63] is a direct evolution of the RESCue-STED [61] technique. If no signal is detected, not only is the STED beam inactive but also the scan skips to the next pixel. This strategy increases the imaging speed by up to 4–5 times compared to RESCue-STED, with a decreased light dose of ~20% [63] in a biological sample compared to conventional STED.

4 Optimized Patterns and Adaptive Detection

The methods described above optimize the scanning strategies to improve image quality and speed while lowering illumination dose. Other methods instead focus on the illumination or detection side.

In the illumination, different spatial distributions of the STED beam have been explored. In particular, the use of one-dimensional depletion patterns instead of a two-dimensional doughnut shape allows for a more efficient depletion (due to steeper minima and consequently lower saturation light). A two-dimensional resolution improvement is then obtained by recording one-dimensional high-resolution

images at multiple angles of the depletion pattern. For this reason, the strategy is called tomographic STED [64].

In the detection, by measuring the arrival time of photons at the detection site, information regarding their origin across the PSF can be inferred. Gated-STED is an implementation mainly applied to STED using CW depletion lasers [65]. The lower peak powers of CW lasers decreases the efficiency of stimulated emission and thus the STED beam has not had time to induce sufficient suppression of fluorescence at early times after the excitation pulse. With time-gated detection as in gated-STED, only the photons arriving in the later parts of the lifetime window and thus increasingly from the central parts of the PSF are used to construct the image, increasing the resolution. A similar concept is used in the SPLIT-STED implementation, where a phasor analysis is used to separate "high-resolution photons" (mainly from the central parts of the PSF) from "low-resolution photons" (mainly from the outer parts of the PSF) based on photon arrival times [66–68]. Optimized detection and photon assignment schemes like these enable high-resolution imaging to be performed with lower and less perturbing illumination intensities. Alternatively, the strategies can be used to improve the resolution without the need of increasing the illumination dose.

One additional strategy to compensate for photobleaching, therefore allowing long recording time, focuses on the probe and more specifically the labelling strategy. Combining the PAINT (Point Accumulation for Imaging in Nanoscale Topography) [69] and the STED approach, fluorogenic labels that transiently bind to their target structure can be used to obtain a constant exchange of labels between the solution and the target structure [70, 71]. As a consequence, the photobleached population of fluorophores is constantly exchanged with a new set of bright fluorophores, allowing prolonged STED recordings. The potential of this approach was demonstrated by extended timelapse and volumetric recording without degradation of the image quality. Alternatively, a photobleaching-immune approach has been developed for the study of the extracellular space of the brain with 3D STED microscopy. The entire extracellular fluid is labeled with a fluorescent marker to enable super-resolution shadow imaging (SUSHI [72]) of the extracellular space in living organotypic brain slices, and thus negative imaging of the complete cellular outlines. The large volume and continuous refreshing of fluorescent labels makes the technique unaffected by photobleaching and protected from phototoxicity since phototoxic molecules are produced outside of the cells.

5 Parallelization

Another way of increasing the imaging speed, especially for large FOV images, is through parallelization of the illumination and read-out (Fig. 5). In coordinate-targeted switching techniques, the parallelized acquisition means that the illumination confines and probes the fluorescence of the sample in multiple points at the same time. Using different types of light patterns, arrays of sharply confined emitting

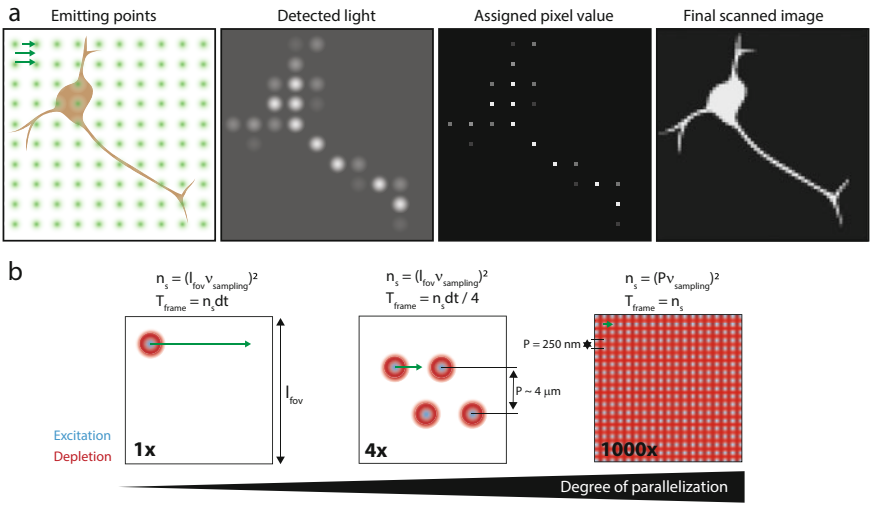

Fig. 5 From point scanning to parallelization. (**a**) Representation of a parallelized workflow. Parallelization of coordinate-targeted switching techniques relies on creating multiple emitting points in the sample that are imaged onto an extended sensor. If the emitting points are sufficiently far apart, the emission from the different points can be independently quantified and assigned to the corresponding pixel in the final image. Thanks to the parallelization, the number of scanning steps can be greatly reduced. (**b**) From a single scanning point, the degree of parallelization can be gradually increased by multiplexing the foci and doughnut patterns or pushed to the limit using large patterns generating tightly packed emitting spots separated only by a distance just above the diffraction limit

points are generated, each probing a spatially separate part of the sample. For arrays of emitting points covering the whole FOV, the scanning time is then decoupled from the FOV and instead defined by the distance between the individual illumination points. The array of emitting points needs to be read out at the same time but in spatially distinct pixels achievable either with multiple point detectors or using large camera sensors. The emission from each point is quantified by measuring the recorded fluorescence signal, which will be assigned to the corresponding pixel in the final image. Parallelized scanning has been proposed and implemented both in STED and RESOLFT systems.

The different characteristics of STED and RESOLFT introduce different challenges and limitations regarding the extent of parallelization. In STED, the scale of achievable parallelization is limited by the high intensity required for efficient depletion, while in RESOLFT the lower intensity allows for extended parallelization of the illumination. In both STED and RESOLFT, the temporal resolution of parallelized systems is to a certain extent limited by the current camera technology. Read-out times of state-of-the-art cameras are currently limited to a few milliseconds for the often required megapixel frames. In STED microscopy, the required pixel dwell time is usually only a few tens of microseconds. In point-scanning systems with practically instantaneous read-out, the pixel dwell time is thus usually also a

few tens of microseconds. In a highly parallelized STED system, though, every scan step requires a camera frame to be read out, resulting instead in pixel dwell times on the millisecond time scale. Much of the gain from the reduced number of scan steps is therefore lost with the increased pixel dwell time. On the other hand, the switching cycle in RESOLFT systems requires several hundreds of microseconds or even milliseconds to achieve the on-state confinement in each scan step. The camera read-out time, therefore, increases the pixel dwell time by a relatively low amount and parallelization of RESOLFT systems can thus give a vast improvement in imaging speed compared to point-scanning systems. Nonetheless, even a parallelized RESOLFT system only outperforms a point-scanning STED system in terms of imaging speed if the side of a squared imaged region surpasses ~5–10 μm.

The use of cameras as detectors adds some additional complexity, but also offers more possibilities to the processing of the detected signal. In contrast to a single-point detector, which inevitably integrates all photons on the photosensitive area, a camera can capture images of the intensity distribution detected. This allows for different types of digital pinholing or more advanced statistical analysis of the detected signal.

5.1 Parallelized STED

STED has been demonstrated with different approaches and degrees of parallelization [73–75]. With four illumination spots at a distance of 5.7 μm, the first implementation could achieve only a moderate degree of parallelization. The moderate degree of parallelization however allowed for the continued use of point detectors, leading to an increased recording speed by four times compared to a single-point-scanning approach [74] (Fig. 5a). This however comes at the expense of system complexity and scalability of the approach. This together gives a four times faster system able to image structures down to ~35 nm (Fig. 5b, center).

A significantly higher degree of parallelization was achieved by introducing a new STED beam pattern exhibiting zero-intensity points over a large region and at a periodicity of 290 nm [73, 75] (Fig. 5b, right). Each zero-intensity point allows for highly confined emission creating a large array of emitting points. To detect the highly parallelized emission, point detectors are substituted by a camera sensor. As discussed, the slower reading time of a camera compared to a point detector in a STED microscope limits the pixel dwell time. For this reason, the 1,000-fold parallelization achieved in the implementations based on large interference patterns for depletion can increase the recording speed to seconds, but not to the theoretical recording time of 100 frames per second (potentially achievable considering the pixel dwell times of STED). Furthermore, to achieve such speeds, the extension of the parallelization requires high laser intensities to induce stimulated emission, demanding powerful laser sources or a smaller number of foci. The use of a spatial light modulator to create the optical lattice for the depletion could reach ~70 nm

resolution over $3 \times 3\ \mu m^2$ FOV [73]. Improvement on the laser source (low repetition rate and high pulse energy) could extend the FOV to 20 μm in diameter [75]. The continued development of laser and detector technology may further extend the current limit of parallelized STED.

5.2 *Parallelized RESOLFT*

In contrast to STED microscopy, the molecular switching required for RESOLFT microscopy leads to pixel dwell times on the order of hundreds of microseconds to milliseconds. Since this is on par with the speed of fast exposure times using state-of-the-art sCMOS cameras, significant gains can be made in terms of imaging speed by parallelizing the raster-scanned acquisition of RESOLFT microscopes. Many different implementations of parallelized RESOLFT exist, all aiming at achieving high degrees of parallelization by using illumination patterns covering large areas of the sample (up to $100 \times 100\ \mu m^2$) [76–79].

5.2.1 Widefield-RESOLFT

The implementation of parallelized RESOLFT that gives the highest degree of parallelization uses homogeneous widefield illumination for the on-switching and read-out step of the pulse scheme and a superposition of orthogonal sinusoidal patterns in the off-switching step to achieve the confined emission. This implementation is termed Widefield-RESOLFT (wf-RESOLFT) [76] and is illustrated in Fig. 6. The distribution of confined emitting points in wf-RESOLFT is solely

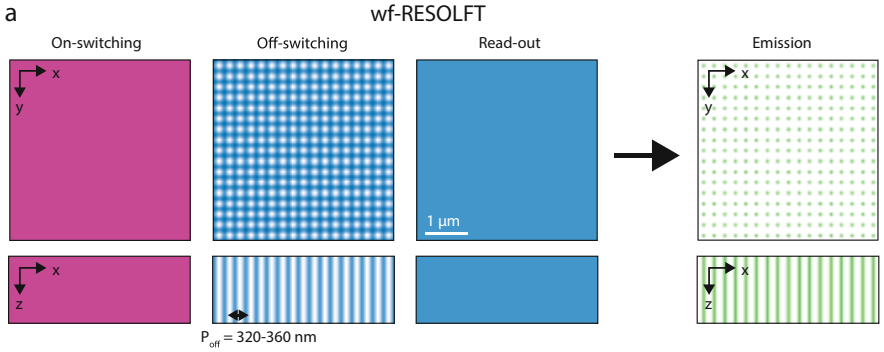

Fig. 6 wf-RESOLFT patterns. A high degree of parallelization can be achieved by switching on the whole FOV with a widefield illumination. A patterned illumination exhibiting an array of zeros switches off everything except the fluorophores residing in these zero-intensity points. A final widefield illumination excites fluorescence from the remaining on-state fluorophores. Scale bar: 1 μm

determined by the geometry of the off-switching pattern. To achieve sharply confined on-state points in a short time, it is beneficial to use an off-switching pattern with a steep intensity gradient surrounding the intensity zeroes. The shorter the periodicity of the pattern, the lower the intensity at its peaks is needed to achieve the same confinement [75, 80]. As an additional benefit, the contraction of the periodicity translates into an increased speed of recording, although it comes with the drawback of cross-talk between neighboring emitting spots, whose PSFs will start to overlap in the detected image. Overlapping PSFs on a parallelized detector can be separated using computational unmixing or deconvolution algorithms [76, 77], although the presence of noise will quickly deteriorate the image quality. In practice, this limits the accessibility of the technique to bright and flat samples, while axially extended samples where out-of-focus emission has a larger contribution or signal-to-noise is low are difficult to image. Balancing all these aspects, wf-RESOLFT has been implemented using off-switching patterns with a periodicity, P, of 320–360 nm [46, 76, 77], and with a massive improvement in throughput covering a FOV of 100 μm in diameter. Overall, the time of the RESOLFT pulse scheme multiplied by n_s (now defined as $(P/d_s)^2$ instead of $(l_{fov}/d_s)^2$ as in point scanning) leads to a frame time of around 3 s for a $l_{fov} = 100 \times 100\ \mu m^2$. The low illumination powers required for RESOLFT imaging makes wf-RESOLFT a suitable method for acquiring timelapse recordings of large and flat samples.

5.2.2 MoNaLISA or Multifoci Parallelized RESOLFT

To extend the parallelized approach to thicker 3D samples, the influence of out-of-focus emitting regions and the cross-talk between in-focus emitters needs to be minimized or eliminated. This has been achieved by independently modulating the periodicity of the on-switching and read-out illumination, named P_{on} and P_{ro}, from the one of the off-switching illumination, P_{off}, in the RESOLFT pulse scheme (Fig. 7). In practice, this can be done by creating an array of intensity maxima in the focal plane with the use of microlenses and relay optics. Spatially modulated on-switching light switches on primarily the fluorophores residing at these points (Fig. 7). The co-alignment of the intensity maxima of the on-switching multifoci with every minimum of the off-switching array generates sharply confined nanosized regions of fluorophores (Fig. 7). The additional multifoci read-out pattern co-aligned with the on-switching pattern is used to excite fluorescence from these spatially confined on-state molecules. The multifoci pattern in the on-switching and read-out step not only allows for better signal detection from in-focus emitters but also gives the system improved optical sectioning. Indeed, the non-overlapping PSFs of the emitting points allow for digital pinholing to discard most of the out-of-focus signal. Additionally, the combination of illumination patterns creates emission primarily from the focal plane of the system (Fig. 8a), both due to the two-step process of

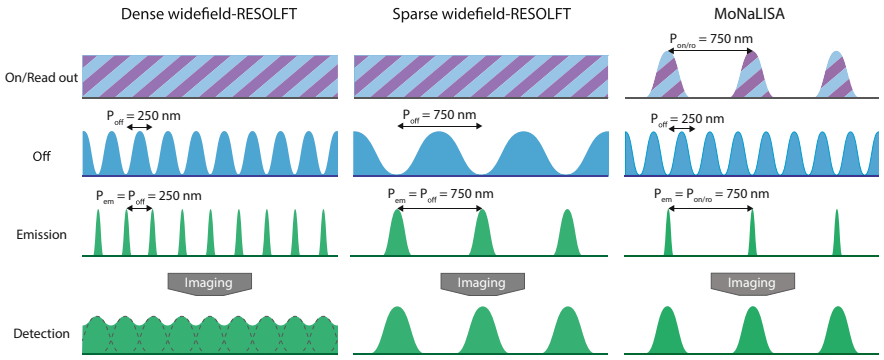

Fig. 7 wf-RESOLFT and MoNaLISA. The wf-RESOLFT configuration forces a trade-off between the ability of the off-switching pattern to confine the emission and the distance between adjacent emitting points. An off-switching pattern with high modulation will create sharply confined emitting spots, but at such a short distance from each other that they will be hard to distinguish in the diffraction-limited detection. Relaxing the modulation of the off-switching pattern will bring the emitting points further apart but will also compromise the confinement of the emitting spots. The MoNaLISA scheme alleviates this problem by decoupling the modulation of the off-switching pattern from the distance between adjacent emitting spots

on-switching and read-out but also since much of the out of focus on-switched molecules will be switched off by the off-switching pattern.

Having decoupled periodicities ($P_{on} = P_{ro} \neq P_{off}$) allows shrinking P_{off} down to the diffraction limit ~250 nm, without affecting the cross-talk of the emitting spots, which is defined by P_{on}. The MoNaLISA (Molecular Nanoscale Live Imaging with Sectioning Ability [78]) system delivers fast high-resolution imaging of living cells by balancing the trade-off between imaging speed and image quality and by providing optical sectioning through axially confined emission and digital pinholing. Fields of view of 50 × 50 μm^2 are recorded at around 1 Hz inside the three-dimensional structures of the cell. The enhanced contrast gained by the full integration of the emitting volume enables the use of fast and resistant RSFPs that due to lower brightness are generally difficult to image in other parallelized systems (Fig. 8b). Dim signal, like the endogenous level of expression of vimentin tagged with rsEGFP2 protein, can be visualized thanks to the improved contrast of MoNaLISA. In Fig. 8c, the contrast and resolution of MoNaLISA images are compared with widefield and enhanced confocal (using multifoci arrays without the off-switching pattern) images of the same structures.

5.2.3 3D Parallelized RESOLFT

Although the multifoci arrays used in the MoNaLISA microscope provide optical sectioning abilities, the axial resolution is still diffraction limited. The off-switching pattern used in these implementations does not provide any additional confinement

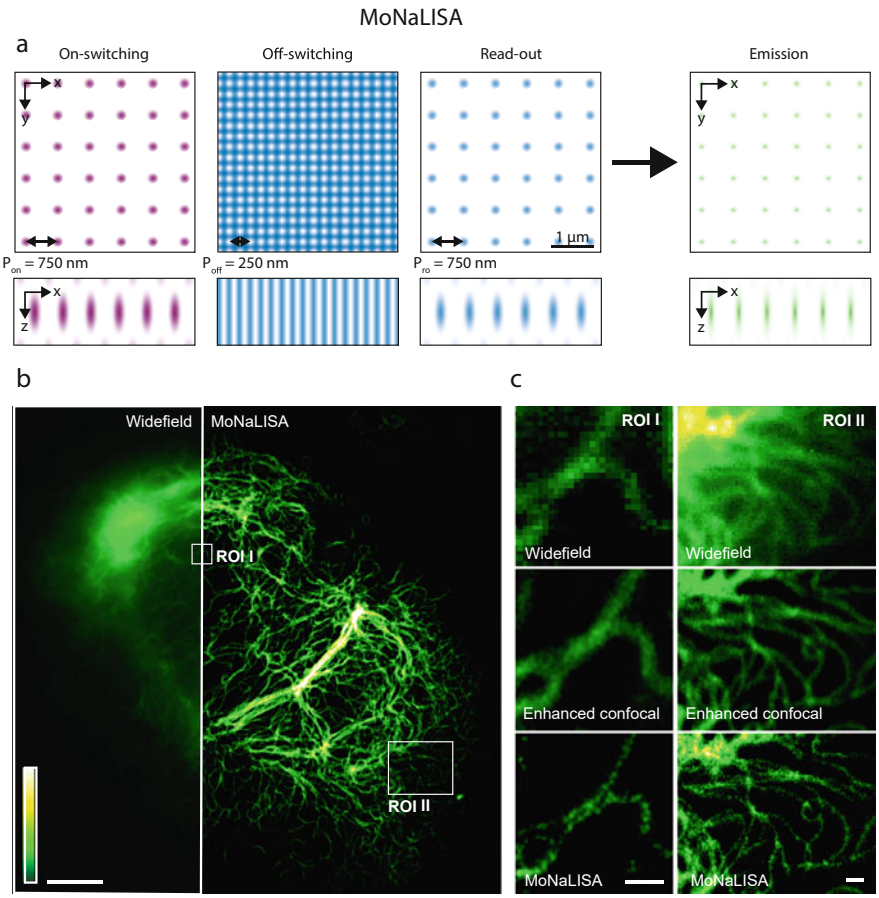

Fig. 8 MoNaLISA patterns and data. (**a**) In the MoNaLISA scheme, additional patterns are added into the pulse scheme causing the on-switching and read-out light to be confined to a sparser subset of zero-points in the off-switching pattern and also inducing an axially confined emission. (**b**) Comparison of a traditional widefield image with MoNaLISA image of U2OS cell endogenously expressing Vimentin-rsEGFP2. Scale bar: 5 µm. (**c**) Zoom-ins of ROI I and II showing a comparison of the resolution and contrast achieved with widefield imaging, enhanced confocal (using multifoci arrays without the off-switching pattern), and the full MoNaLISA scheme. Scale bars: 500 nm. Image adapted from Masullo et al. [78]

along the axial direction. Three-dimensional super-resolution has however been demonstrated using a more complex off-switching pattern that exhibits three-dimensionally confined zero-intensity points [79]. An example of a 3D-confining pattern is shown in Fig. 9a. This pattern, in combination with the multifoci array used for on-switching and read-out, creates emitting volumes that are confined in all three spatial dimensions. Probing the spatial distribution of fluorophores in 3D

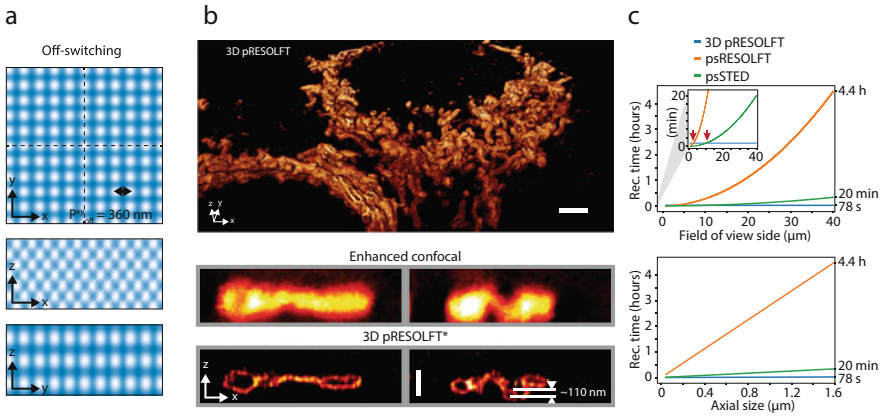

Fig. 9 3D pRESOLFT pattern and data. (**a**) Extension to 3D super-resolution can be achieved by creating an off-switching pattern that exhibits zero-volumes confined in all three dimensions, creating a 2D lattice structure in both the x–y, x–z and y–z planes. (**b**) Full volumetric recording of a mitochondrial network, together with an x–z slice of a single mitochondria compared with an enhanced confocal recording of the same structure showing the drastically improved resolution in all dimensions. Cells are U2OS expressing rsEGFP2-Omp25. Star (*) denotes deconvolved data. Scale bars: 2 μm (top) and 500 nm (bottom). (**c**) Graphs showing approximate imaging time taken for volumetric imaging using psRESOLFT, psSTED, and 3D pRESOLFT. The top graph assumes a fixed axial size of 1.6 μm with increasing lateral FOV. The bottom graph assumes a fixed 40 × 40 μm^2 lateral FOV with increasing axial size. Calculations assume standard pixel dwell times of the different techniques (psSTED: 30 μs, psRESOLFT: 400 μs, 3D pRESOLFT: 6 ms) and a scan step size of 50 nm

requires the sample to be raster scanned along the x-, y- and z-dimension with a scanning step satisfying the Nyquist-Shannon sampling criterion.

Examples of improved axial resolution on a point-scanning architecture have been proved by utilizing interference between two opposite objectives (isoSTED [81, 82], 4Pi-RESOLFT [83]) or using axial depletion patterns in a single objective configuration (3DSTED [9, 84]), shrinking the PSF down to 30–50 nm. This 3D parallelized RESOLFT (3D pRESOLFT) implementation has been shown to achieve a spatial resolution below 80 nm in all three dimensions. As such, it is a powerful tool for measuring the lateral and axial spatial distribution of proteins in micrometer thick sections of axially extended samples as shown in volumetric images of mitochondria of U2OS cells presented by Bodén et al. [79] and shown in Fig. 9b. Parallelization on a volumetric recording translates into a 200-fold improvement in the speed of recording, comparing the same RESOLFT dwell time (from 4.4 h for point-scanning RESOLFT to 78 s in 3D pRESOLFT, Fig. 9c).

5.3 *Digital Pinholing of Camera Data*

When multiple emitting points are imaged onto a camera, a consecutive step is needed to quantify the emissions from the emitting points and assign them to the correct pixels in the final image. The most straightforward approach is the use of a binary mask on the camera frame, aligned to the a priori knowledge of the geometry of the emitting points. If the emitting points are sufficiently far apart compared to the diffraction limit, this approach is the digital analogy to the use of a physical pinhole in a point-scanning system. This approach has been used in wf-RESOLFT systems with a Gaussian pinhole function instead of a binary mask [76]. If the images of the emitting points are too close to each other so that their respective PSFs overlap, very small pinholes need to be used in order to minimize cross-talk (around one-fifth of the Airy disc). Alternatively, the cross-talk can be unmixed by defining the problem as a system of linear equations to be solved through least-squares minimization or maximum likelihood estimations [75, 77]. High cross-talk between emitting regions reduces the total signal extractable from each spot. Alternatively, when the emitting points are non-overlapping, as in MoNaLISA and 3D pRESOLFT systems, they can be considered independent from each other. Therefore, each camera region can then be processed individually and the signal can be fully extracted and separated from the background contribution.

6 STED and RESOLFT for Live-Cell Imaging

STED and RESOLFT microscopy are versatile imaging tools that can be used for a plethora of different imaging applications in material and biological sciences including plants, bacterial, and mammalian systems. Their contribution to these disciplines is extensively covered in many recent reviews [85–87]. Here we limited our attention to the new strategies introduced in coordinate-targeted nanoscopy to push their ability toward live-cell imaging at the nanoscale. Within this goal, three aspects assume a central role: temporal resolution, phototoxicity, and cell accessibility. We summarized the techniques described in the previous paragraphs according to these metrics to give a comparative view of them (Table 1).

Since biological processes take place on many time scales, from milliseconds to hours, following sub-second dynamics without sacrificing spatial resolution or the overall cellular context represents an important challenge in biological imaging. STED microscopy, providing instantaneous nanoscale confinement, reaches extremely short pixel dwell times ($<$100 μs). Though parallelized approaches have been demonstrated, the most common implementation of STED still uses a single scanning point due to the requirements on power density and limitations imposed by current camera technology. This intrinsically links the temporal resolution of the technique to the size of the FOV recorded. For smaller fields of view, STED systems can reach tens of milliseconds temporal resolution enabling the study of fast

Table 1 Comparison of the super-resolution deterministic strategies for increased live-cell imaging compatibility

	Category	Technique name	Live-cell compatibility	Pixel dwell time	Frame time (n_s = 20 nm)	Light dose	Lateral resolution	Axial resolution	Specialized fluorophores	Key features	Ref
POINT SCANNING	Conventional	psSTED	Low	10–100 µs	20 µm in 10–100 s	50–900 kJ/cm^2 (775 nm)	~20–50 nm	~ 40–100 nm	No		
		psRESOLFT	Medium	100–500 µs	20 µm in 1–10 min	0.2 kJ/cm^2 (4, 405 nm)	~20–50 nm	~ 40–100 nm	Yes		
	Adaptive scanning	RESCue	Medium	✗	20 µm in 10–100 s*	8 fold lower	50 nm	170 nm	No	Lower light dose	61
		Fast-RESCue	High	✓	20 µm in 2–20 s*	5–6 fold lower	50 nm	Not shown	No	Lower light dose, faster scanning	63
		MINFIELD	Medium	✗	n/a	10–500 fold lower	20 nm	90 nm	No	Lower bleaching in small FOV	90
		DyMIN	Medium	✗	20 µm in 10–100 s	~ 20 fold lower	29 nm	70 nm	No	Lower light dose	14
		SmartRESOLFT	High	✓	20 µm in 50–130 s	5 fold lower	40 nm	Not shown	Yes	Lower light dose, faster scanning	13
	Adaptive detection	SPLIT-STED	Medium	✗	20 µm in 10–100 s	2 fold lower	60 nm	Not shown	No	Lower light dose	66,67
	Optimized pattern	TomoSTED	Medium	✗	20 µm in 10–100 s	~ 2.5 fold lower	65 nm	Not shown	No	Lower light dose	64
	Refreshable probe/labeling	SUSHI	Medium	✗	20 µm in 10–100 s	Same	50 m	200 nm	Yes	Prolonged imaging	72
		Exchangeable dyes STED	Medium	✗	20 µm in 10–100 s	Same	60 nm	240 nm	Yes	Prolonged imaging	70
	Isotropic PSF	isoSTED	Low	✗	20 µm in 10–100 s (1–8 min)	Same	50–60 nm	50–60 nm	No	Isotropic 3D resolution	81,82
		4Pi-RESOLFT	Medium	✗	20 µm in 1–10 min (1–8 h)	Same	30–50 nm	30–50 nm	Yes	Isotropic 3D resolution	83
PARALLELIZED	STED-type	4-points STED	Low	✓	2.5–25 s	Same	35 nm	400–500 nm	No	Faster scanning	74
		1000-points STED	Low	✗	20 µm in ~10 s	15 fold lower	30 nm	Not shown	No	Faster imaging on extended FOV	75
		SLM STED	Medium	✗	2.8 µm in ~180 ms	Lower**	70 nm	Not shown	No	Faster imaging	73
	RESOLFT-type	wfRESOLFT	High	✗	100 µm in ~ 6 s	Lower**	80 nm	Not shown	Yes	Faster imaging on extended FOV	76
		MoNaLISA	High	✗	50 µm in ~ 5 s	Lower**	55 nm	320 nm	Yes	Faster volumetric imaging	78
		3D pRESOLFT	High	✗	40 µm in ~ 8 s (7 min)	Lower**	70 nm	80 nm	Yes	Isotropic and faster imaging on extended FOV	79

(continued)

Table 1 (continued)

Table. Comparison of the super-resolution deterministic strategies for increased live-cell imaging compatibility.

The different techniques covered in the chapter are compared on the basis of several parameters. **Live-cell compatibility**: For live-cell compatibility we chose a scale from low to high, in which we considered both speed and light dose. In particular, fast and low-illumination techniques are considered as highly live-cell compatible (high), while slower and light-demanding techniques are identified as minimally live compatible (low). If only one of the two parameters is addressed by the technological development introduced, we define them as medium live-cell compatible. **Pixel dwell time:** Some of the reported techniques are based on shortening the average dwell time either based on decisions performed independently on each scanning step or multiplexing the reading in each scan step (✓), others maintain the dwell time fixed (✗). As a reference the typical dwell time for STED and RESOLFT are reported. **Frame time**: The time required to scan an image depends on the area to be scanned, the scan step, and the dwell time. For point-scanning approaches the area to be scanned corresponds to the FOV of interest, optical aberrations generally limit it to around 50 × 50 μm^2, with reported optimized scanning up to 100 x 100 μm^2 for STED microscopy[91]. The speed for the reported point-scanning techniques is assessed on a 20 × 20 μm^2 FOV considering a scan step of 20 nm and a pixel dwell time of 10 – 100 μs for STED and 100–500 μs for RESOLFT. For the highly parallelized approaches, where the area scanned is decoupled from the FOV and only dependent on the periodicity of the pattern, the frame time and the achieved maximum FOV (throughput of the parallelization) is reported. For the techniques that have isotropic resolution (isoSTED, piRESOLFT, 3D pRESOLFT) the time needed to record a volume of 20 × 20 × 1 μm^3 with a scan step of 20 nm in all directions is reported. **Light dose:** Light doses are presented as comparative values, where RESOLFT implementations are compared to psRESOFLT and STED implementations to psSTED. The relative decrease reported is the one stated in the original publications. **Lateral and axial resolution:** The estimated resolution is reported in all dimensions if stated in the original publication. **Specialized fluorophores:** Some of the techniques rely on the use of specific labels or specialized labeling strategies. In particular, for RESOLFT, reversibly switchable fluorophores are required, while a transient binding is essential for STED techniques with exchangeable dyes. For SUSHI, a negative volumetric staining is used, instead of a direct link to a structure. **Key features:** Quick summary of the aspects that define the technique. **Ref:** Reference where the technique is reported and characterized.

*Frame time for (Fast-)RESCue STED is calculated considering a dwell time of 100 μs, while in the original publication a dwell time of 400 μs is generally considered, that would result in a frame time of 10 min and 2 min for RESCue and Fast-RESCue, respectively.

**The geometrical consideration on the repetitive off pattern vs single doughnut shape reported in Bergermann et al[75] translate to a varying degree to the other types of highly parallelized techniques, although the different implementations use different light patterns and spatial distributions for the different wavelengths in use. This is reflected in a complex change of the light dose to the sample, for an in-depth analysis on phototoxicity and the influence of the different wavelengths we refer to the original publications.

processes in small localized regions. RESOLFT on the contrary has intrinsically slower dwell time (>100 μs) but offers more modularity in recording strategy. The ability to work with lower intensities allows moving from single-point scanning to extended parallelized recordings.

The nanoscale resolution for both techniques also increases the need for sensitivity. Higher resolution ultimately means a decrease in the emitting volume and the number of fluorophores contributing to the signal. The universal nature of stimulated emission provides a great variety of fluorophores to choose from. Especially useful are the bright and photostable dyes that can push the resolving ability toward 20–30 nm. For RESOLFT, instead, the primary type of labels to date are the RSFPs that often offer a limited photon budget highly dependent on the illumination condition being used. When the system under study is dynamic, it is not only crucial to achieve high resolution on a snapshot of the sample, but also to describe its time evolution. The need for stable fluorophores to meet this demand is a common requirement among super-resolution techniques, as that photostability ultimately limits the sampling and the time window available.

Considerations on light damage in live-cell experiments are of great importance and a complex topic where many factors come into play. High irradiance on cells generally increases the risk of phototoxicity but how the light is distributed in space and time on the sample is also crucial to the effect. Slow scanning (i.e., long dwell time) induces more pronounced stress on the cells compared to fast scanning (i.e., short dwell time, compensated by line or frame averaging to reach a similar contrast [88]). The level of resolution achievable in the deterministic approach is tuned by the intensity of the off switching beam, which allows tuning of the power used according to the desired resolution. The smart scanning approaches push this concept of adaptability to the sample further by actively investigating the space and introducing a decision in the recording. In each step, a decision is taken whether to use the STED beam or not, or whether to stay or to move. Another parameter that can influence the level of phototoxicity in the sample is the wavelength of light in use, with red-shifted light being less toxic to the cells. Moving the STED beam toward the red has been crucial to increasing its live-cell compatibility. For RESOLFT almost all reported switching mechanisms involve the use of UV–violet light at different doses depending on the specific photophysics in use. The complex photophysics of some red RSFPs allows moving away from this requirement and completing the whole switching cycle with light above 500 nm. Active research into new switching mechanisms can further help to move away from this requirement. Especially for negatively switching RSFPs, the UV light dose is minimal and does not preclude imaging at different scales, from adherent cells to full organisms like *Drosophila* [89] or *C. Elegans* [13]. In general, RESOLFT microscopy with its significantly lower illumination intensities is a technique aimed primarily at live-cell imaging, allowing prolonged recordings of living cells and tissues. However, the performance of the technique is highly dependent on the use of a few select fluorescent markers. A broader adaptation to a wider range of biological questions is dependent on the continued development of new probes and illumination schemes.

7 Challenges and Outlooks

Coordinate-targeted switching approaches to super-resolution microscopy have in the last 20 years moved from being a niche technique, available only to highly specialized labs and for selected biological applications to being a technique widely used in life science institutes around the world. The psSTED microscope, for example, is today a workhorse in many imaging facilities. This is largely due to the versatility of the technique, easily extendable to multicolor and able to achieve high resolution in fixed, thin and thick samples. It also benefits from the possibility to use conventional dyes and to be added as an extra module onto a standard confocal microscope. However, for applications requiring long-term and minimally invasive monitoring of living cells, point-scanning systems often fall short due to the time taken to scan the image with a single point and the energy applied by focused light. Novel smart and adaptive scanning systems partially overcome this issue by optimizing the scanning trajectory and illumination sequence. Development in this direction is already available in some commercial microscopes and open-source initiative. RESOLFT microscopes are also commercialized, to some extent also with the parallelized recording (i.e., wfRESOLFT), even if these are less present in imaging facilities. The lack of commercial RESOLFT systems is likely due to the need for specific probes and that the technique is mainly targeted at live-cell imaging. Multicolor RESOLFT, though feasible, is also more challenging due to the need for multiple laser wavelengths for each RSFP requiring multiple lasers for multicolor imaging. Finally, the use of RESOLFT for live-cell imaging is still fairly recent, with the first successful results emerging only about 10 years ago.

Going from a single-point-scanning microscope to a parallelized system adds significant optical complexity to the setup but can provide orders of magnitude improvements in imaging speed and decrease of illumination dose. The added optical complexity of parallelized schemes arises particularly when different patterned illuminations are used in multiple steps of the illumination scheme to accommodate the need of specialized photoswitchable probes. In MoNaLISA and 3D pRESOLFT systems, three different illumination patterns need to be crafted and co-aligned to each other in order to generate high-quality images. Additionally, as in single-point-scanning approaches, the quality of the zeros in the off-pattern needs to be close to perfect in order to achieve sharp on-state confinement. Refractive index variations or other optical imperfections in the sample may cause aberrations to the illuminating beams distorting the geometry or degrading the quality of the zero-intensity points. The issues become more severe when imaging deeper into the sample. Imaging tens of micrometers inside tissue is thus challenging even with the improved optical sectioning provided by these systems. Future implementation of adaptive optics may provide solutions to restore the quality of the wave front inside the sample enabling high-resolution imaging further inside tissues. Creating patterns with controllable shape and maintained quality throughout thicker samples may also allow for even faster volumetric imaging with parallelization also along the axial dimensions.

Highly parallelized imaging schemes often rely on cameras for detection. Although they provide the properties that make this type of imaging possible, they also limit the systems in some aspects. One such limitation comes from the relatively long time required to read out the data from a camera frame. Even state-of-the-art sCMOS cameras require several milliseconds to read out a full camera frame (~4 MP). Since every scan step in a parallelized scanning sequence requires a frame to be read out, the camera read-out time is often a major bottleneck in the data acquisition scheme. In parallelized RESOLFT schemes, the camera read-out time usually accounts for about 20–50% of the pixel dwell time [55, 78, 79]. In parallelized STED systems, this relative time may be significantly higher due to the fast timescale of stimulated emission allowing for microsecond integration times. Cameras also introduce other challenges stemming from their noise properties. Not only do they exhibit non-zero amounts of read-out noise (not present in APDs), but the use of cameras can also introduce additional pixel-dependent noise. Considerations need to be taken to handles all these aspects and future camera and detector development will likely contribute greatly to further push these techniques in terms of image quality and speed.

Another challenge likely to be undertaken is to extend these super-resolution techniques to multi-channel or multicolor imaging. STED microscopy is commonly implemented in multicolor imaging of up to four colors [92]. RESOLFT, however, is still limited to the library of existing RSFPs. Finding multiple spectrally separated RSFPs with switching kinetics that allow for fast imaging remains a challenge. Additionally, if the different RSFPs are switched by different wavelengths, the illumination patterns need to be created and aligned in multiple beam paths adding again to the complexity of the optical system. Other ways to generate multicolor RESOLFT images have been proposed as being preferable, for example, by separating different RSFP labels by their switching kinetics [93, 94]. This has the benefit of requiring only one spectral illumination and detection channel. However, it still requires RSFPs that differ not in spectral but in photoswitching behavior, more specifically fast and slow off-switching kinetics. As a consequence, the imaging speed is limited by the switching speed of the slower switcher. Utilizing both spectral and dynamic parameters to separate channels may allow future implementations with three or more separable channels. More in general, the development of new switchable proteins in different regions of the spectra, with different photophysical behavior and with an added sensing module (e.g., calcium [95, 96] or pH [97]) will likely pave the way for new technical innovations and applications.

In this chapter, we covered the strategies used in deterministic super-resolution techniques to reach higher compatibility toward fast live-cell imaging. The deterministic coordinate-targeted switching approaches compose a subset of super-resolution fluorescence microscopy techniques. The distinction between coordinate-targeted approaches and stochastic localization techniques has however narrowed as techniques are emerging combining stochastic switching with scanning systems and illumination patterns. The concept was first introduced with the MINFLUX technique [98–100] and has been further adapted in other forms and to other applications [101–104]. The successful utilization of well-designed

illumination strategies together with accurate knowledge of photophysical behavior will likely be the key to further refinement of optical systems for the interrogation of biological structures and dynamics. The continued improvement of such systems is essential for the advancement of biological research in the life sciences.

References

1. Abbe E (1873) Beiträge zur Theorie des Mikroskops und der mikroskopischen Wahrnehmung. Arch Mikrosk Anat 9(1):413–468
2. Hell SW, Kroug M (1995) Ground-state-depletion fluorscence microscopy: a concept for breaking the diffraction resolution limit. Appl Phys B Lasers Opt 60:495–497
3. Hell SW, Wichmann J (1994) Breaking the diffraction resolution limit by stimulated emission: stimulated-emission-depletion fluorescence microscopy. Opt Lett 19:780–782
4. Hell SW (2007) Far-field optical nanoscopy. Science 316:1153–1158
5. Hess ST, Girirajan TPK, Mason MD (2006) Ultra-high resolution imaging by fluorescence photoactivation localization microscopy. Biophys J 91:4258–4272
6. Rust MJ, Bates M, Zhuang XW (2006) Sub-diffraction-limit imaging by stochastic optical reconstruction microscopy (STORM). Nat Methods 3:793–795
7. Betzig E et al (2006) Imaging intracellular fluorescent proteins at nanometer resolution. Science 313:1642–1645
8. Hell SW, Wichman J (1994) Breaking the diffraction resolution limit by stimulated emission: stimulated-emission-depletion fluorescence microscopy. Opt Lett 19:780–782
9. Klar TA, Jakobs S, Dyba M, Egner A, Hell SW (2000) Fluorescence microscopy with diffraction resolution barrier broken by stimulated emission. Proc Natl Acad Sci 97:8206–8210
10. Hofmann M, Eggeling C, Jakobs S, Hell SW (2005) Breaking the diffraction barrier in fluorescence microscopy at low light intensities by using reversibly photoswitchable proteins. Proc Natl Acad Sci 102:17565–17569
11. Grotjohann T et al (2011) Diffraction-unlimited all-optical imaging and writing with a photochromic GFP. Nature 478:204–208
12. Grotjohann T et al (2012) rsEGFP2 enables fast RESOLFT nanoscopy of living cells. eLife 2012:1–14
13. Dreier J et al (2019) Smart scanning for low-illumination and fast RESOLFT nanoscopy in vivo. Nat Commun 10:556
14. Heine J et al (2017) Adaptive-illumination STED nanoscopy. Proc Natl Acad Sci 114:9797–9802
15. Sahl SJ, Schönle A, Hell SW (2019) Fluorescence microscopy with nanometer resolution: nanoscale resolution in far-field fluorescence microscopy. In: Hawkes PW, Spence JCH (eds) Springer handbook of microscopy. Springer, pp 1089–1143. https://doi.org/10.1007/978-3-030-00069-1_22
16. Wang L, Frei MS, Salim A, Johnsson K (2019) Small-molecule fluorescent probes for live-cell super-resolution microscopy. J Am Chem Soc 141:2770–2781
17. Stockhammer A, Bottanelli F (2021) Appreciating the small things in life: STED microscopy in living cells. J Phys D Appl Phys 54:033001
18. Jeong S, Widengren J, Lee J-C (2021) Fluorescent probes for STED optical nanoscopy. Nano 12:21
19. Bordenave MD, Balzarotti F, Stefani FD, Hell SW (2016) STED nanoscopy with wavelengths at the emission maximum. J Phys D Appl Phys 49:365102
20. Vicidomini G, Moneron G, Eggeling C, Rittweger E, Hell SW (2012) STED with wavelengths closer to the emission maximum. Opt Express 20:5225

21. Hotta J et al (2010) Spectroscopic rationale for efficient stimulated-emission depletion microscopy fluorophores. J Am Chem Soc 132:5021–5023
22. Vicidomini G, Bianchini P, Diaspro A (2018) STED super-resolved microscopy. Nat Methods 15:173–182
23. Zheng Q, Lavis LD (2017) Development of photostable fluorophores for molecular imaging. Curr Opin Chem Biol 39:32–38
24. Tønnesen J, Nadrigny F, Willig KI, Wedlich-Söldner R, Nägerl UV (2011) Two-color STED microscopy of living synapses using a single laser-beam pair. Biophys J 101:2545–2552
25. Matlashov ME et al (2020) A set of monomeric near-infrared fluorescent proteins for multicolor imaging across scales. Nat Commun 11:1–12
26. Willig KI, Stiel AC, Brakemann T, Jakobs S, Hell SW (2011) Dual-label STED nanoscopy of living cells using photochromism. Nano Lett 11:3970–3973
27. Han KY et al (2009) Three-dimensional stimulated emission depletion microscopy of nitrogen-vacancy centers in diamond using continuous-wave light. Nano Lett 9:3323–3329
28. Lesoine MD et al (2013) Subdiffraction, luminescence-depletion imaging of isolated, giant, CdSe/CdS nanocrystal quantum dots. J Phys Chem C 117:3662–3667
29. Liu Y et al (2017) Amplified stimulated emission in upconversion nanoparticles for super-resolution nanoscopy. Nature 543:229–233
30. Tosheva KL, Yuan Y, Matos Pereira P, Culley S, Henriques R (2020) Between life and death: strategies to reduce phototoxicity in super-resolution microscopy. J Phys D Appl Phys 53: 163001
31. Wäldchen S, Lehmann J, Klein T, van de Linde S, Sauer M (2015) Light-induced cell damage in live-cell super-resolution microscopy. Sci Rep 5:15348
32. Erdmann RS et al (2019) Labeling strategies matter for super-resolution microscopy: a comparison between HaloTags and SNAP-tags. Cell Chem Biol 26:584–592.e6
33. Keppler A et al (2003) A general method for the covalent labeling of fusion proteins with small molecules in vivo. Nat Biotechnol 21:86–89
34. Los GV et al (2008) HaloTag: a novel protein labeling technology for cell imaging and protein analysis. ACS Chem Biol 3:373–382
35. Gautier A et al (2008) An engineered protein tag for multiprotein labeling in living cells. Chem Biol 15:128–136
36. Arsić A, Hagemann C, Stajković N, Schubert T, Nikić-Spiegel I (2022) Minimal genetically encoded tags for fluorescent protein labeling in living neurons. Nat Commun 13:314
37. Bottanelli F et al (2016) Two-colour live-cell nanoscale imaging of intracellular targets. Nat Commun 7:1–5
38. Moneron G et al (2010) Fast STED microscopy with continuous wave fiber lasers. Opt Express 18:1302
39. Schneider J et al (2015) Ultrafast, temporally stochastic STED nanoscopy of millisecond dynamics. Nat Methods 12:827–830
40. Shcherbakova DM, Sengupta P, Lippincott-Schwartz J, Verkhusha VV (2014) Photocontrollable fluorescent proteins for superresolution imaging. Annu Rev Biophys 43: 303–329
41. Nienhaus K, Nienhaus GU (2016) Chromophore photophysics and dynamics in fluorescent proteins of the GFP family. J Phys Condens Matter 28:443001
42. Stiel AC et al (2007) 1.8 Å bright-state structure of the reversibly switchable fluorescent protein Dronpa guides the generation of fast switching variants. Biochem J 402:35–42
43. Duwé S et al (2015) Expression-enhanced fluorescent proteins based on enhanced green fluorescent protein for super-resolution microscopy. ACS Nano 9:9528–9541
44. El Khatib M, Martins A, Bourgeois D, Colletier JP, Adam V (2016) Rational design of ultrastable and reversibly photoswitchable fluorescent proteins for super-resolution imaging of the bacterial periplasm. Sci Rep 6:1–12
45. Wang S et al (2018) GMars-T enabling multimodal subdiffraction structural and functional fluorescence imaging in live cells. Anal Chem 90:6626–6634

46. Wang S et al (2016) GMars-Q enables long-term live-cell parallelized reversible saturable optical fluorescence transitions nanoscopy. ACS Nano 10:9136–9144
47. Shinoda H et al (2018) Acid-tolerant monomeric GFP from Olindias formosa. Cell Chem Biol 25:330–338.e7
48. Gregor C et al (2018) Novel reversibly switchable fluorescent proteins for RESOLFT and STED nanoscopy engineered from the bacterial photoreceptor YtvA. Sci Rep 8:2724
49. Andresen M et al (2008) Photoswitchable fluorescent proteins enable monochromatic multilabel imaging and dual color fluorescence nanoscopy. Nat Biotechnol 26:1035–1040
50. Tiwari DK et al (2015) A fast- and positively photoswitchable fluorescent protein for ultralow-laser-power RESOLFT nanoscopy. Nat Methods 12:515–518
51. Konen T et al (2021) The positive switching fluorescent protein Padron2 enables live-cell reversible saturable optical linear fluorescence transitions (RESOLFT) nanoscopy without sequential illumination steps. ACS Nano 15:9509–9521
52. Jensen NA et al (2014) Coordinate-targeted and coordinate-stochastic super-resolution microscopy with the reversibly switchable fluorescent protein dreiklang. ChemPhysChem 15:756–762
53. Brakemann T et al (2011) A reversibly photoswitchable GFP-like protein with fluorescence excitation decoupled from switching. Nat Biotechnol 29:942–950
54. Lavoie-Cardinal F et al (2014) Two-color RESOLFT nanoscopy with green and red fluorescent photochromic proteins. ChemPhysChem 15:655–663
55. Pennacchietti F et al (2018) Fast reversibly photoswitching red fluorescent proteins for live-cell RESOLFT nanoscopy. Nat Methods 15:601–604
56. Kwon J et al (2015) RESOLFT nanoscopy with photoswitchable organic fluorophores. Sci Rep 5:1–8
57. Nevskyi O et al (2018) Fluorescent diarylethene photoswitches—a universal tool for super-resolution microscopy in nanostructured materials. Small 14:1–12
58. Uno K et al (2021) Turn-on mode diarylethenes for bioconjugation and fluorescence microscopy of cellular structures. Proc Natl Acad Sci 118:e2100165118
59. Roubinet B et al (2016) Carboxylated photoswitchable diarylethenes for biolabeling and super-resolution RESOLFT microscopy. Angew Chem Int Ed 55:15429–15433
60. Frawley AT et al (2020) Super-resolution RESOLFT microscopy of lipid bilayers using a fluorophore-switch dyad. Chem Sci 11:8955–8960
61. Staudt T et al (2011) Far-field optical nanoscopy with reduced number of state transition cycles. Opt Express 19:5644
62. Göttfert F et al (2017) Strong signal increase in STED fluorescence microscopy by imaging regions of subdiffraction extent. Proc Natl Acad Sci 114:2125–2130
63. Vinçon B, Geisler C, Egner A (2020) Pixel hopping enables fast STED nanoscopy at low light dose. Opt Express 28:4516
64. Krüger J-R, Keller-Findeisen J, Geisler C, Egner A (2020) Tomographic STED microscopy. Biomed Opt Express 11:3139
65. Vicidomini G et al (2011) Sharper low-power STED nanoscopy by time gating. Nat Methods 8:571–573
66. Lanzanò L et al (2015) Encoding and decoding spatio-temporal information for super-resolution microscopy. Nat Commun 6:6701
67. Tortarolo G et al (2019) Photon-separation to enhance the spatial resolution of pulsed STED microscopy. Nanoscale 11:1754–1761
68. Wang L et al (2018) Resolution improvement in STED super-resolution microscopy at low power using a phasor plot approach. Nanoscale 10:16252–16260
69. Sharonov A, Hochstrasser RM (2006) Wide-field subdiffraction imaging by accumulated binding of diffusing probes. Proc Natl Acad Sci 103:18911–18916
70. Spahn C, Grimm JB, Lavis LD, Lampe M, Heilemann M (2019) Whole-cell, 3D, and multicolor STED imaging with exchangeable fluorophores. Nano Lett 19:500–505

71. Urban NT, Willig KI, Hell SW, Nägerl UV (2011) STED nanoscopy of actin dynamics in synapses deep inside living brain slices. Biophys J 101:1277–1284
72. Tønnesen J, Inavalli VVGK, Nägerl UV (2018) Super-resolution imaging of the extracellular space in living brain tissue. Cell 172:1108–1121.e15
73. Yang B, Przybilla F, Mestre M, Trebbia J-B, Lounis B (2014) Large parallelization of STED nanoscopy using optical lattices. Opt Express 22:5581
74. Bingen P, Reuss M, Engelhardt J, Hell SW (2011) Parallelized STED fluorescence nanoscopy. Opt Express 19:23716–23716
75. Bergermann F, Alber L, Sahl SJ, Engelhardt J, Hell SW (2015) 2000-fold parallelized dual-color STED fluorescence nanoscopy. Opt Express 23:211–211
76. Chmyrov A et al (2013) Nanoscopy with more than 100,000 'doughnuts'. Nat Methods 10: 737–740
77. Chmyrov A et al (2017) Achromatic light patterning and improved image reconstruction for parallelized RESOLFT nanoscopy. Sci Rep 7:44619
78. Masullo LA et al (2018) Enhanced photon collection enables four dimensional fluorescence nanoscopy of living systems. Nat Commun 9:1–9
79. Bodén A et al (2021) Volumetric live cell imaging with three-dimensional parallelized RESOLFT microscopy. Nat Biotechnol 39(5):609–618. https://doi.org/10.1038/s41587-020-00779-2
80. Rego EH et al (2012) Nonlinear structured-illumination microscopy with a photoswitchable protein reveals cellular structures at 50-nm resolution. Proc Natl Acad Sci U S A 109:1–9
81. Curdt F et al (2015) isoSTED nanoscopy with intrinsic beam alignment. Opt Express 23:30891
82. Siegmund R, Werner F, Jakobs S, Geisler C, Egner A (2021) isoSTED microscopy with water-immersion lenses and background reduction. Biophys J 120:3303–3314
83. Böhm U, Hell SW, Schmidt R (2016) 4Pi-RESOLFT nanoscopy. Nat Commun 7:10504
84. Harke B, Ullal CK, Keller J, Hell SW (2008) Three-dimensional nanoscopy of colloidal crystals. Nano Lett 8:1309–1313
85. Bond C, Santiago-Ruiz AN, Tang Q, Lakadamyali M (2022) Technological advances in super-resolution microscopy to study cellular processes. Mol Cell 82:315–332
86. Sahl SJ, Hell SW, Jakobs S (2017) Fluorescence nanoscopy in cell biology. Nat Rev Mol Cell Biol 18:685–701
87. Maglione M, Sigrist SJ (2013) Seeing the forest tree by tree: super-resolution light microscopy meets the neurosciences. Nat Neurosci 16:790–797
88. Kilian N et al (2018) Assessing photodamage in live-cell STED microscopy. Nat Methods 15: 755–756
89. Schnorrenberg S et al (2016) In vivo super-resolution RESOLFT microscopy of Drosophila melanogaster. elife 5:e15567
90. Göttfert F et al (2017) Strong signal increase in STED fluorescence microscopy by imaging regions of subdiffraction extent. Proc Natl Acad Sci 114:2125–2130
91. Alvelid J, Testa I (2020) Stable stimulated emission depletion imaging of extended sample regions. J Phys D Appl Phys 53:24001
92. Willig KI, Wegner W, Müller A, Clavet-Fournier V, Steffens H (2021) Multi-label in vivo STED microscopy by parallelized switching of reversibly switchable fluorescent proteins. Cell Rep 35:109192
93. Testa I, D'Este E, Urban NT, Balzarotti F, Hell SW (2015) Dual channel RESOLFT nanoscopy by using fluorescent state kinetics. Nano Lett 15:103–106
94. Valenta H et al (2021) Separation of spectrally overlapping fluorophores using intra-exposure excitation modulation. Biophys Rep 1:100026
95. Mishra K et al (2022) Genetically encoded photo-switchable molecular sensors for optoacoustic and super-resolution imaging. Nat Biotechnol 40(4):598–605. https://doi.org/10.1038/s41587-021-01100-5

96. Gielen V et al (2020) Absolute measurement of cellular activities using photochromic single-fluorophore biosensors. http://biorxiv.org/lookup/doi/10.1101/2020.10.29.360214. https://doi.org/10.1101/2020.10.29.360214
97. Seidel ZP, Wang JCK, Riegler J, York AG, Ingaramo M (2021) Relaxation sensors. Zenodo. https://doi.org/10.5281/zenodo.5810930
98. Balzarotti F et al (2017) Nanometer resolution imaging and tracking of fluorescent molecules with minimal photon fluxes. Science 355(6325):606–612
99. Eilers Y, Ta H, Gwosch KC, Balzarotti F, Hell SW (2018) MINFLUX monitors rapid molecular jumps with superior spatiotemporal resolution. Proc Natl Acad Sci 115:6117–6122
100. Gwosch KC et al (2020) MINFLUX nanoscopy delivers multicolor nanometer 3D-resolution in (living) cells. Nat Methods 17(2):217–224. https://doi.org/10.1101/734251
101. Cnossen J et al (2020) Localization microscopy at doubled precision with patterned illumination. Nat Methods 17(1):59–63. https://doi.org/10.1101/554337
102. Reymond L et al (2019) SIMPLE: structured illumination based point localization estimator with enhanced precision. Opt Express 27:24578
103. Jouchet P et al (2021) Nanometric axial localization of single fluorescent molecules with modulated excitation. Nat Photonics 15:297–304
104. Gu L et al (2019) Molecular resolution imaging by repetitive optical selective exposure. Nat Methods 16:1114–1118